JAERI-M
7432

RADIATIVE COOLING IN THE OUTER EDGE OF A TOKAMAK PLASMA BY LOW-Z IMPURITIES

December 1977

Masayuki NAGAMI

日本原子力研究所
Japan Atomic Energy Research Institute

JAERI-M 7432

Radiative Cooling in the Outer Edge of a Tokamak Plasma by Low-Z Impurities

Masayuki NAGAMI
Division of Thermonuclear Fusion Research,
Tokai Research Establishment, JAERI

(Received November 15, 1977)

Radiative cooling capabilities of partially stripped low-Z impurities (carbon, oxygen and neon) in a tokamak plasma have been studied. In DIVA-sized tokamak, with the most probable diffusion model (neoclassical diffusion superposed by anomalous diffusion) of recycling impurities, the radial density distributions of individual ionization states are calculated and the loss power due to line radiation is evaluated. In the outer edge region of the discharge, the impurities recycling from and to the wall deviate from the local coronal equiliblium and the radiation power is greater by a factor of about 20 than estimated from the coronal equilibrium state. Width of this intensive cooling layer is determined by the ionization energy of Li-like state, so that neon gives the largest layer in the outer edge of the discharge with the highest radiation intensity.

Keywords: Radiative Cooling, Outer Edge, DIVA Tokamak, Recycling, Line Radiation, Coronal Equilibrium, Li-like State, Low-Z Impurity

JAERI－M 7432

軽元素不純物によるトカマク・プラズマの周辺領域での冷却効果

日本原子力研究所東海研究所核融合研究部
永見　正幸

（１９７７年１１月１５日受理）

トカマク・プラズマ中に存在する軽元素不純物による周辺領域の冷却効果を炭素，酸素，ネオンについて調べた。壁とリサイクリングを行う不純物イオンの各電離状態の小半径方向の密度分布を新古典多成分イオン拡散と，プロトンの閉じ込めを支配する異常拡散とを考慮した輸送モデルで計算し，その結果を用いて線放射損失の分布を求めた。壁と強くリサイクリングを行う周辺領域では不純物イオンはコロナ平衡状態に比べ低い電離状態で存在し，その結果放射量はコロナ平衡状態での放射量の数十倍になる。周辺領域でのこの強い放射冷却領域の大きさはリチウム様状態の電離エネルギに依存し，そのために炭素，酸素，ネオンの順に冷却領域が広く，冷却効果が大きくなる。

Contents

目　　次

1. INTRODUCTION

High-Z impurities which cannot be fully stripped in the central region of tokamak plasma emit the intense radiation power, and cause serious effect on the ignition and Lawson conditions of a fusion reactor [1]. Therefore, finding the means to suppress the high-Z impurities below tolerable cocentrations (0.01~0.1 %) is extremely important in determining the feasibility of tokamak reactor.

Recently it is found that intrinsic [ST] or injected low-Z impurity [TFR] has suppressive effect on the contamination by high-Z impurities [2]. This is probably due to the reduction of plasma-wall interaction by radiative cooling at periphery of the discharge [3].

The radiative cooling due to low-Z impurity in the outer edge of tokamak plasma was recently evaluated by Breton et al. [4], using a rather simple impurity diffusion model. Assuming constant inward and outward diffusion velocities, they calculated the radial distribution of radiation power by oxygen impurity in TFR tokamak. This transport model is a rather crude one: the incoming impurities diffuse inward up to the center and then diffuse outward to surface of the discharge. As a result this causes the large radiation power that cannot explain the whole energy balance of the discharge [5].

In this paper, with the most probable diffusion model (neoclassical diffusion superposed by anomalous diffusion) describing the recycling impurities, the radial density distributions of individual ionization levels are calculated and the radiation loss power is evaluated in DIVA-sized tokamak.

Three species of low-Z impurity, i.e. carbon, oxygen and neon are investigated concerning their cooling capability.

2. CALCULATION OF RADIATION LOSS

Number of efforts have been made to evaluate the radiation power emitted from various impurities in coronal equilibrium state. For example, in Ref.[4], the authors calculated the ionization equilibrium of an element that is determined by the equations of steady state coronal equilibrium. The radiation loss was then calculated by adding the emission due to bremsstrahlung, radiative and dielectronic recombination and line radiation.

The present interest is the radiative cooling in the outer edge region of tokamak plasma where the electron temperature is below few hundreds of eV. In this region, the most important radiation mechanism is line radiation due to partially stripped ions. As is presented for oxygen in Ref.[4], the other mechanisms, i.e. radiative and dielectronic recombinations and bremsstrahlung, are one or two order lower than the line radiation power.

Therefore we calculate the radiation power only of line radiation.

If n_z is the density of the ion of charge Z (cm^{-3}), the power density P_r(Watts/cm^3) by line radiation of the ion is

$$P_r = 1.6 \times 10^{-19} n_e n_z \sum_j E_{exj} S_j \ .$$

n_e is the electron density in cm^{-3} and the summation in j is for

Three species of low-Z impurity, i.e. carbon, oxygen and neon are investigated concerning their cooling capability.

2. CALCULATION OF RADIATION LOSS

Number of efforts have been made to evaluate the radiation power emitted from various impurities in coronal equilibrium state. For example, in Ref.[4], the authors calculated the ionization equilibrium of an element that is determined by the equations of steady state coronal equilibrium. The radiation loss was then calculated by adding the emission due to bremsstrahlung, radiative and dielectronic recombination and line radiation.

The present interest is the radiative cooling in the outer edge region of tokamak plasma where the electron temperature is below few hundreds of eV. In this region, the most important radiation mechanism is line radiation due to partially stripped ions. As is presented for oxygen in Ref.[4], the other mechanisms, i.e. radiative and dielectronic recombinations and bremsstrahlung, are one or two order lower than the line radiation power.

Therefore we calculate the radiation power only of line radiation.

If n_z is the density of the ion of charge Z (cm^{-3}), the power density P_r(Watts/cm^3) by line radiation of the ion is

$$P_r = 1.6 \times 10^{-19} n_e n_z \sum_j E_{exj} S_j \ .$$

n_e is the electron density in cm^{-3} and the summation in j is for

all transitions of the ion Z. It is assumed that the lines are emitted by radiative deexcitation of the upper levels of transitions excited from the ground state. E_{ex} is the excitation energy in eV and S_j is the excitation rate coefficient.

We use for S_j the following expression given by Mewe [6]

$$S_j = 1.58 \times 10^{-5} \frac{f_i \bar{g}}{\sqrt{T_e}\, E_{exj}} \exp(- E_{ex}/T_e) \quad ,$$

where T_e is the electron temperature in eV, S_j the absorption oscillation strength and $\bar{g}$ the average effective Gaunt factor.

For the ionization rate coefficients of an impurity ion, we use the expression proposed by Lotz [7]. The radiative and dielectronic recombination rate coefficients are calculated by using the expression given in Ref.[8] and [9].

We first calculate coronal equilibrium states, and using the results of fractional abundances, calculate radiation losses as a function of the electron temperature.

As for the line radiation power, the transitions in the calculation are similar to those by Breton et al.[4], which are shown in the table. E_{ex} and f are taken from the NBS table.

In Fig.1, the ratios, $P/n_e n_z$, are shown for carbon, oxygen and neon as a function of the electron temperature. Also the same relation given by Tarter [10] for oxygen is shown in the same figure.

In these curves, maxima in the lower side of the electron temperature correspond to regions in which transitions among levels having the same principal quantum number are strongly excited.

The minima in the curves occur when closed shell configurations are predominant (He-like state), so that the ion cannot be excited at that temperature. On the higher side of electron temperature, there are small maxima due to excitation of 1s-np transitions. As is shown in Ref.[4], at higher temperatures, the contribution by dielectronic recombination and bremsstrahlung is no negligible. The corresponding deviations from the results of Tarter is found in the present calculation at high temperature. However, on the lower side of temperature, Tarter's result and ours are in agreement.

3. RADIAL TRANSPORT MODEL OF IMPURITY IONS

To evaluate the radial distributions of radiation power, calculation of the radial density distributions of individual ionization levels is necessary. We calculate them with a radial transport model that have yielded good fit to the experimental transient radial diffusion of pulsively injected carbon impurity [11]. That is, the transport of impurity ion is described by neoclassical diffusion superposed by anomalous diffusion of protons.

For neoclassical impurity ion transport, we use the expression by Tuda and Tanaka [12]. That is, the cross field ion flux $\Gamma_{\alpha\beta}$ of species α (averaged over a magnetic surface) due to the friction with ions of species β is given as

$$Z_\alpha \Gamma_{\alpha\beta} = - \frac{m_{\alpha\beta} n_\alpha}{\tau_{\alpha\beta}} \frac{(1+2q^2)T}{e^2 B^2} \left(\frac{1}{z_\alpha n_\alpha} \frac{\partial n_\alpha}{\partial r} - \frac{1}{z_\beta n_\beta} \frac{\partial n_\beta}{\partial r} \right) ,$$

where the collision time has the form

The minima in the curves occur when closed shell configurations are predominant (He-like state), so that the ion cannot be excited at that temperature. On the higher side of electron temperature, there are small maxima due to excitation of 1s-np transitions. As is shown in Ref.[4], at higher temperatures, the contribution by dielectronic recombination and bremsstrahlung is no negligible. The corresponding deviations from the results of Tarter is found in the present calculation at high temperature. However, on the lower side of temperature, Tarter's result and ours are in agreement.

3. RADIAL TRANSPORT MODEL OF IMPURITY IONS

To evaluate the radial distributions of radiation power, calculation of the radial density distributions of individual ionization levels is necessary. We calculate them with a radial transport model that have yielded good fit to the experimental transient radial diffusion of pulsively injected carbon impurity [11]. That is, the transport of impurity ion is described by neoclassical diffusion superposed by anomalous diffusion of protons.

For neoclassical impurity ion transport, we use the expression by Tuda and Tanaka [12]. That is, the cross field ion flux $\Gamma_{\alpha\beta}$ of species α (averaged over a magnetic surface) due to the friction with ions of species β is given as

$$z_\alpha \Gamma_{\alpha\beta} = - \frac{m_{\alpha\beta} n_\alpha}{\tau_{\alpha\beta}} \frac{(1+2q^2)T}{e^2 B^2} \left(\frac{1}{z_\alpha n_\alpha} \frac{\partial n_\alpha}{\partial r} - \frac{1}{z_\beta n_\beta} \frac{\partial n_\beta}{\partial r} \right) ,$$

where the collision time has the form

$$\tau_{\alpha\beta} = \frac{3\sqrt{m_{\alpha\beta}}\, T^{3/2}}{4\sqrt{2\pi}\, z_\alpha^2 z_\beta^2 n_\beta e^4 \ell n\Lambda} , \qquad m_{\alpha\beta} = \frac{m_\alpha m_\beta}{m_\alpha + m_\beta} ,$$

n, m, z are the density, mass and charge number of each species. T, B, q are the proton temperature, the toroidal magnetic field and the safety factor, respectively. The different ion species are assumed to have the temperatures equal to the proton temperature.

The conservation equation for the density of proton n_p is

$$\frac{\partial n_p}{\partial t} = -\frac{1}{r}\frac{\partial}{\partial r}(r\Gamma_p) + n_e n_o I_p ,$$

$$\Gamma_p = \Gamma_p^a + \sum_k \Gamma_{pk} ,$$

and that for the density of impurity ions of jth ionized level n_j is

$$\frac{\partial n_j}{\partial t} = -\frac{1}{r}\frac{\partial}{\partial r}(r\Gamma_j) + n_e[I_{j-1}n_{j-1} - (I_j + R_j)n_j + I_{j+1}n_{j+1}] ,$$

$$\Gamma_j = \Gamma_j^a + \Gamma_{jp} + \sum_k \Gamma_{jk} ,$$

where I_p and I_j are the electron impact ionization rate coefficients of hydrogen and impurity respectively and R_j is the radiative and dielectronic recombination rate coefficient. The electron density n_e is then given by

$$n_e = n_p + \sum_z Z n_z .$$

In these equations, Γ_p^a, Γ_j^a are the anomalous diffusion flux; Γ_{pk} and Γ_{jp} the diffusion fluxes due to collisions between protons and impurity ions; Γ_{jk} the diffusion flux due to the collisions between impurity ions of the charge j and impurity ions of the charge k.

The influxes of hydrogen and impurity atoms are determined assuming perfect recycling at the wall, and the density distributions in the discharge, n_0 and n_1 are calculated by Dnestrovskii's formula [13] with correction for geometrical effects (cylindrical plasma).

The boundary conditions are

$$\frac{\partial n_p}{\partial r} = \frac{\partial n_j}{\partial r} = 0 \qquad \text{at } r = 0 \ ,$$

$$n_p = 2 \times 10^{11} \text{ cm}^{-3}, \quad n_j = 0 \text{ at } r = r_w \ ,$$

where r_w is the wall radius.

The coupled conservation equations are integrated by the fully implicit Crank - Nicholson method [14].

4. RADIATIVE COOLING IN THE OUTER EDGE DUE TO RECYCLING IMPURITIES

To study the radiative cooling in the outer edge of a tokamak plasma, we treat the case of DIVA device. The plasma major radius is 60 cm, the minor radius 10 cm, the toroidal field 20 kG, the plasma current 40 kA, the average electron density $3\sim4\times10^{13}$, and the particle confinement time ~2 msec.

Fig.2 shows the model plasma for radial profiles of electron

In these equations, Γ_p^a, Γ_j^a are the anomalous diffusion flux; Γ_{pk} and Γ_{jp} the diffusion fluxes due to collisions between protons and impurity ions; Γ_{jk} the diffusion flux due to the collisions between impurity ions of the charge j and impurity ions of the charge k.

The influxes of hydrogen and impurity atoms are determined assuming perfect recycling at the wall, and the density distributions in the discharge, n_0 and n_1 are calculated by Dnestrovskii's formula [13] with correction for geometrical effects (cylindrical plasma).

The boundary conditions are

$$\frac{\partial n_p}{\partial r} = \frac{\partial n_j}{\partial r} = 0 \qquad \text{at } r = 0 \ ,$$

$$n_p = 2 \times 10^{11} \text{ cm}^{-3}, \quad n_j = 0 \text{ at } r = r_w \ ,$$

where r_w is the wall radius.

The coupled conservation equations are integrated by the fully implicit Crank - Nicholson method [14].

4. RADIATIVE COOLING IN THE OUTER EDGE DUE TO RECYCLING IMPURITIES

To study the radiative cooling in the outer edge of a tokamak plasma, we treat the case of DIVA device. The plasma major radius is 60 cm, the minor radius 10 cm, the toroidal field 20 kG, the plasma current 40 kA, the average electron density $3\sim4\times10^{13}$, and the particle confinement time ~2 msec.

Fig.2 shows the model plasma for radial profiles of electron

and ion temperatures.

In the present calculations, the electron and ion temperatures are constant with time, and the radial density distributions of protons and total impurity ions are initially parabolic. The initial ionization population is determined as a coronal equilibrium state of the electron temperature of 30 eV. Energies of the incoming neutral hydrogen and impurity atom are taken as 10 eV.

4.1 Calculation of the radial density distribution of impurity ions

For the anomalous diffusion coefficient D_a, we apply the simple expression presented by Mercier [15],

$$D_a = C(1 + 1.6\ q^2)\ \nu_{ei}\rho_{eT}^2$$

where ν_{ei} and ρ_{eT} are the electron-ion collision frequency and the electron ramor-radius in the toroidal magnetic field respectively. We take 200 for C, and in the region where $q < 1$, the value is multiplied by a factor of 5 to simulate the enhanced diffusion due to the sawtooth oscillation. Then the radial fluxes due to the anomalous processes are

$$\Gamma_p^a = - D_a \frac{\partial n_p}{\partial r} \quad , \quad \Gamma_j^a = - D_a \frac{\partial n_j}{\partial r} \quad .$$

Fig.3 shows calculated radial density distributions of individual ionization levels at 6 msec, which are almost in steady state. In the three respective species, we assume a contamination 3 % the total number of protons. Calculated results for the three species show that the particle confinement

times of protons and impurity ions are 1.6-1.8 msec and 1.9-3.9 msec respectively.

As indicated in the figure, carbon and oxygen are dominantly in fully ionized state in the central region of the discharge, and in partially ionized states below Li-like state in the outer edge region.

The calculation code used takes into account up to the ninth ionization level, so that for neon, the treatment is up to He-like state, NeIX. The results show that the self-spreading anomalous diffusion gives relatively broad radial density profiles, compared with those by Breton et al.

4.2 Radiative cooling

Fig.4 shows calculated radial distributions of raidation power. The intensive radiation is caused by partially stripped ions below Li-like state present in the outer edge although the population and the electron density are rather small. Therefore, width of the intensive radiation is determined by ionization energy of Li-like state for a given radial electron temperature profile. The ionization energy of the Li-like state is 239 eV for neon, 138 eV for oxygen, and 64 eV for carbon, so that for a given electron temperature profile, neon has the largest width. Since the total radiation power is attributed mainly to that from the outer edge region, the results show that neon emits the largest power: 64 kW for neon, 33 kW for oxygen and 17 kW for carbon.

In Fig.5 for oxygen, the width of intensive radiative cooling is shown for three different electron temperature profiles, narrow (a) to broad (c). The results show that the existence of

Li-like state is limited in the region of electron temperatures below about 150 eV.

Besides the results of width of the intensive radiative cooling, it should be noted that, in the present transport model, the narrow radial profile of electron temperature gives poor confinement of the impurity ion ((a) 2.3 msec, (b) 3.2 msec, (c) 4.1 msec) and cause more intensive recycling.

Enhancement of the incoming flux of neutral impurity atoms due to the poor confinement of impurity ions results in increase of the partially stripped ions below Li-like state leading to rize of the radiation power. On the other hand, good confinement provides the opposite situation, i.e., reduction of the radiation power in the outer edge region.

4.3 Comparison in impurity radiation between coronal and non-coronal calculations

Fig.6 shows the comparison of the present computational result and the coronal calculation given by Tarter in the radial profile of the radiation power. The latter is calculated by using the radial distribution of total ionization levels and of electron temperature.

The finite confinement time of impurity ions in the discharge put the ions in lower ionized levels than coronal equalibrium state, so that the computed result yields a radiation power in a factor of 20 larger in maximum than predicted for the coronal equilibrium state.

To evaluate the actual cooling effect by low-Z impurity, the ionization loss must also be considered.

Incoming neutral impurities are suddenly ionized in the

outer edge region, and successive ionizations continue while the ions diffuse inward or outward in the discharge.

Furthermore the stripped electrons are thermalized up to local electron temperature. Thus the local power loss, P_i, due to ionization of the impurity ion is expressed as

$$P_i = 1.6 \times 10^{-19} n_e \sum_z n_z S_{ion} [E_{ion} + \frac{3}{2} T_e] \ (W/cm^3) \quad ,$$

where S_{ion} and E_{ion} are the ionization rate coefficient and the ionization porential in eV respectively. In Fig.6, the calculated radial distribution of ionization loss for oxygen is shown. The total power loss is 5.7 kW, which is 17 % of the line radiation power.

5. CONCLUSION

Radiative cooling capabilities of three species of low-Z impurity, i.e. C, O and Ne have been shown in DIVA-sized tokamak.

With the most probable diffusion model (neoclassical diffusion superposed by anomalous diffusion) of recycling impurities for tokamak plasma, the radial density distributions of individual ionization levels were calculated and using the results, the line radiation loss power was evaluated.

Impurities recycling from and to the wall deviate from the local coronal equilibrium state, and yield a radiation power which is larger by a factor of about 20 than estimated from the coronal equilibrium state in the outer edge of the discharge.

Width of this intensive cooling layer is governed by the ionization energy of Li-like state of the impurity, so that neon

outer edge region, and successive ionizations continue while the ions diffuse inward or outward in the discharge.

Furthermore the stripped electrons are thermalized up to local electron temperature. Thus the local power loss, P_i, due to ionization of the impurity ion is expressed as

$$P_i = 1.6 \times 10^{-19} \, n_e \sum_z n_z S_{ion} \, [E_{ion} + \frac{3}{2} T_e] \ (W/cm^3) \quad ,$$

where S_{ion} and E_{ion} are the ionization rate coefficient and the ionization porential in eV respectively. In Fig.6, the calculated radial distribution of ionization loss for oxygen is shown. The total power loss is 5.7 kW, which is 17 % of the line radiation power.

5. CONCLUSION

Radiative cooling capabilities of three species of low-Z impurity, i.e. C, O and Ne have been shown in DIVA-sized tokamak.

With the most probable diffusion model (neoclassical diffusion superposed by anomalous diffusion) of recycling impurities for tokamak plasma, the radial density distributions of individual ionization levels were calculated and using the results, the line radiation loss power was evaluated.

Impurities recycling from and to the wall deviate from the local coronal equilibrium state, and yield a radiation power which is larger by a factor of about 20 than estimated from the coronal equilibrium state in the outer edge of the discharge.

Width of this intensive cooling layer is governed by the ionization energy of Li-like state of the impurity, so that neon

gives the largest layer with the highest radiation intensity.

ACKNOWLEDGEMENT

The author would like to thank members of the DIVA group for discussions, and is also grateful to Drs. Y. Tanaka, Y. Obata and S. Mori for their encouragement.

REFERENCES

[1] JENSEN, R.V., POST, D.E., and JASSBY, D.L., PPPL-1350 (1977).

[2] MESERVER, E., BRETZ, N., DIMOCK, D., and HINNOV, E., MATT-1175 (1975).
TFR GROUP, EUR-CEA-FC-868 (1976).

[3] SHIMOMURA, Y., Nucl. Fusion 17 (1977) 626.

[4] BRETON, C., DE MICHELIS, C., and MATTIOLI, M., EUR-CEA-FC-822 (1976).

[5] TFR GROUP, EUR-CEA-FC-892 (1977).

[6] MEWE, R., Astron. and Astrophys. 20 (1972) 215.

[7] LOTZ, W., Zeitschrift für Physik 216 (1968) 241.

[8] VON GOELER, S., STODIEK, W., EUBANK, H., FISHMAN, H., GREBENSHCHIKOV, S., and HINNOV, E., Nucl. Fusion 15 (1975) 301.

[9] BURGESS, A., Astrophys. J., 141 (1965) 1588.

[10] TARTER, C.B., UCRL-78119 (1976).

[11] NAGAMI, M., et al. "Pulsed Methane Injection Experiment on DIVA", to be published.

[12] TUDA, T., and TANAKA, M., JAERI-M 5376 (1973).

[13] DNESTROVSKII, Yu. N., KOSTOMAROV, D.P., PAVLOVA, N.L., Atomraya Energiya, 32 (1972) 301.

[14] HOGAN, J.T., ORNL-TM-5153 (1975).

[15] MERCIER, C., EUR-CEA-FC 812 (1976).

TABLE

Iso. el. seq.	Transitions Configurations	Terms	Iso. el. seq.	Transitions Configurations	Terms
H	1s -2s	$^2S-^2S$	Be	$2s^2$ -2s2p	$^1S-^1P$
	1s -2p	$^2S-^2P$		$2s^2$ -2s3s	$^1S-^1S$
	1s -3s	$^2S-^2S$		$2s^2$ -2s3p	$^1S-^1P$
	1s -3p	$^2S-^2P$		$2s^2$ -2s3d	$^1S-^1D$
	1s -3d	$^2S-^2D$		$2s^2$ -2s2p	$^1S-^3P$
	1s -4s	$^2S-^2S$		$2s^2$ -2s3s	$^1S-^3S$
	1s -4p	$^2S-^2P$		$2s^2$ -2s3p	$^1S-^3P$
	1s -4d	$^2S-^2D$		$2s^2$ -2s3d	$^1S-^3S$
He	$1s^2$-1s2s	$^1S-^1S$	B	$2s^22p$ $-2s2p^2$	$^2P-^2P$
	$1s^2$-1s2p	$^1S-^1P$			$^2P-^2S$
	$1s^2$-1s3s	$^1S-^1S$			$^2P-^2D$
	$1s^2$-1s3p	$^1S-^1P$			
	$1s^2$-1s3d	$^1S-^1D$			
	$1s^2$-1s2s	$^1S-^3S$	C	$2s^2sp^2$-$2s2p^3$	$^3P-^3P$
	$1s^2$-1s2p	$^1S-^3P$			$^3P-^3S$
	$1s^2$-1s3s	$^1S-^3S$			$^3P-^3D$
	$1s^2$-1s3p	$^1S-^3P$			
	$1s^2$-1s3d	$^1S-^3D$			
			N	$2s^22p^3$-$2s2p^4$	$^4S-^4P$
Li	2s -2p	$^2S-^2P$			
	2s -3s	$^2S-^2S$	O	$2s^22p^4$-$2s^22p^5$	$^3P-^3P$
	2s -3p	$^2S-^2P$			
	2s -3d	$^2S-^2D$			
			F	$2s^22p^5$-$2s2p^6$	$^2P-^2S$

Fig.1 Line radiation power from carbon, oxygen and neon at coronal equilibrium as a function of the electron temperature T_e. Also the radiation loss presented by Tarter for oxygen is shown in the same figure.

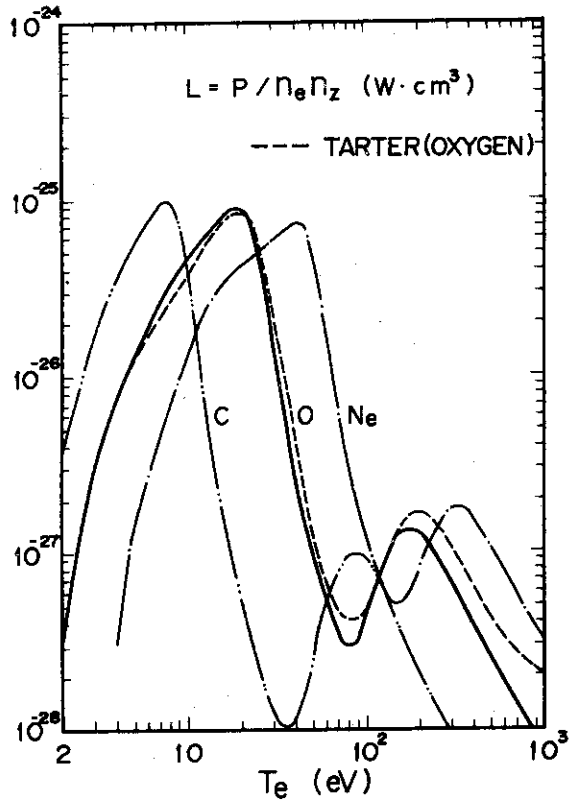

Fig.2 Electron and ion temperature profile, T_e, T_i used in the calculation.

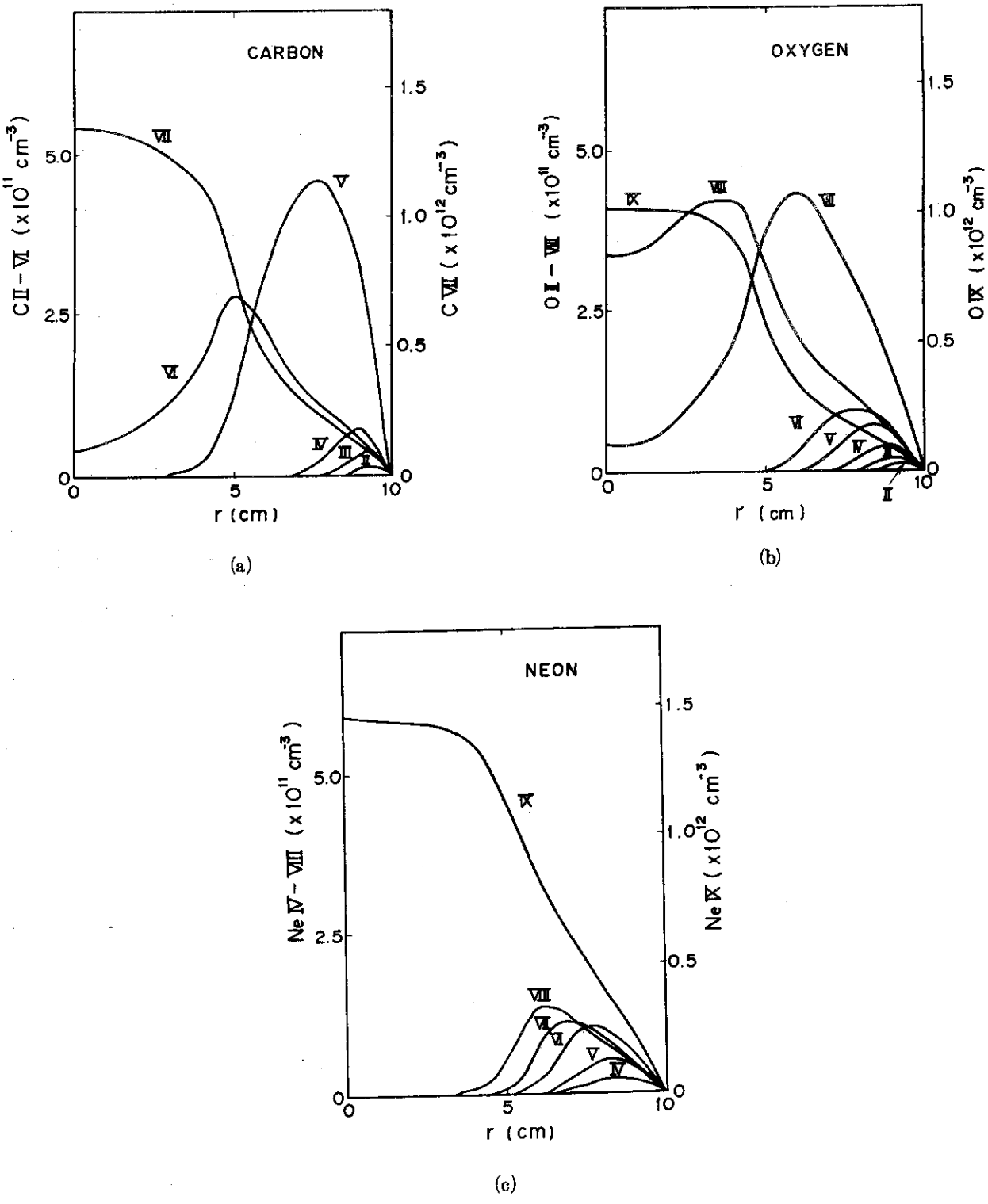

Fig.3 Computed result of the radial density distribution of individual ionization levels; (a) carbon, (b) oxygen, (c) neon. For neon, our treatment is limited up to the He-like state, and the ionization levels below N_eIV are omitted in the figure.

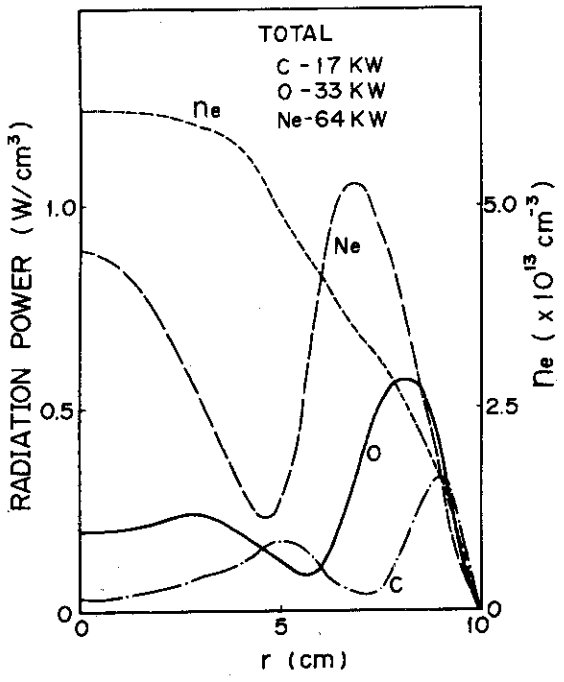

Fig.4 Typical electron density profile, n_e and radial power distributions radiated as line radiation for three low-Z species.

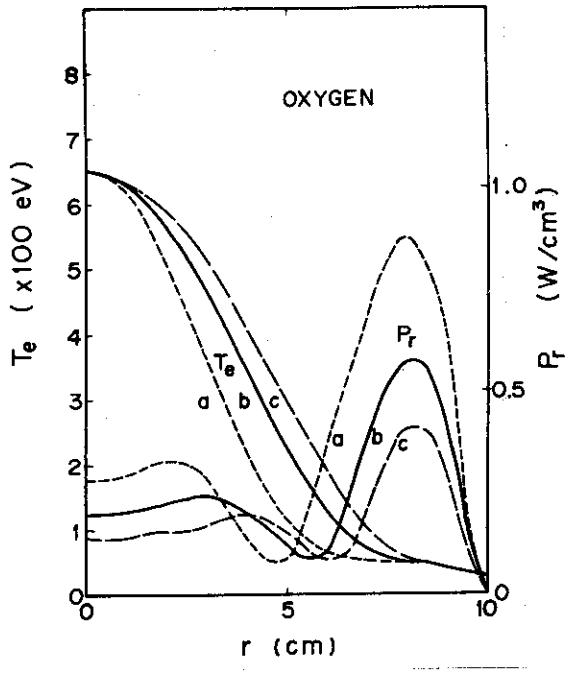

Fig.5 Radial power distributions for different electron temperature profiles for oxygen.

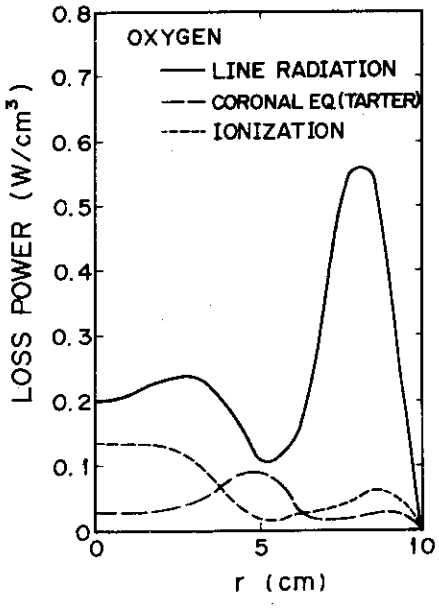

Fig.6 Radial distribution of radiation power from recycling impurities and from impurities of coronal equilibrium (Tarter) for oxygen. Ionization loss profile is also shown.